EXPERIMENTAL AND NUMERICAL STUDY ON AXIAL CRUSHING BEHAVIOUR OF PULTRUDED COMPOSITE TUBES

Sivakumar PALANIVELU[1], Rudy VERHELST[1], Wim VAN PAEPEGEM[1], Joris DEGRIECK[1], Dimitrios KAKOGIANNIS[2], Danny VAN HEMELRIJCK[2], Jan WASTIELS[2], Kathleen DEWOLF[3], John VANTOMME[3]

[1]Department of Mechanical Construction and Production, Ghent University, Sint-Pietersnieuwstraat 41, 9000 Gent, Belgium
[2]Department of Mechanics of Material and Construction, Free University of Brussels, Pleinlaan 2 B-1050 Brussels, Belgium
[3]Royal Military Academy, Civil and Material Engineering Department, Building G, Level 0, 8 Av, Hobbema B-1000, Brussels, Belgium

ABSTRACT

An extensive experimental investigation was carried out to study the energy absorbing characteristics and progressive deformation behavior of unidirectional pultruded composite tubes subjected to an axial impact load. Pultruded square and circular profiles with glass-polyester and glass-vinylester combinations were used to study the specific energy absorption characteristics. Two types of triggering profiles were incorporated to investigate the effect of triggering on energy absorption. All the above combinations were investigated for three impact velocities. The effects of geometry profile, triggering and strain rate on energy absorption of composite tubes were studied in detail. A numerical simulation using finite element method was carried out to assess the energy absorption capability of composite tubes. To model the delamination between the composite plies, a new approach was adopted using cohesive elements. The progressive failure modes and crushing characteristics of the composite tubes are presented. From these studies, the composite tubes can be considered as energy absorbing members for impact applications.

KEYWORDS: Specific energy absorption, triggering, strain rate, progressive failure, cohesive element.

1. INTRODUCTION

The need for a safer vehicle which (i) absorbs energy, (ii) keeps the occupant compartments intact and (iii) ensures tolerable deceleration levels for driver and passengers during the crash event increases due to high speed operation. The above mentioned factors depend upon the design architecture and the materials used in the automobiles. Traditionally different combinations of high strength metal alloys are used in automotive industry to absorb the impact energy for crashworthy applications [1]. The interest on the high strength steels and other metals [2] has been increased to meet the vehicle crashworthiness without increasing the un-laden weight of the vehicle structure and to meet the competitive fuel economy targets.

On the other hand there is a considerable amount of published data available on the energy absorption of composite materials. It is a well-known fact that one can achieve a higher energy absorption compared to metal alloys with the proper design of composite structures. In addition to that, composites have a relative advantage in terms of specific energy absorption, ease of manufacture and maintenance. The energy absorption characteristics of various composite structural elements have been experimentally and numerically studied by several researchers [3-8]. Different cross sections of the tubes are employed to get the maximum energy absorption with the least material investment. However the energy absorption characteristics of the tubes are not only depending on the shape of the tubes [9].

1

Various variables control the energy absorption of the composite structures. The crushing process depends upon mechanical properties of the fibre and the matrix, fiber volume fraction, laminate stacking sequence, fiber architecture and the geometry of the tube. To decelerate the impactor, failed tubes exhibit transverse shearing, lamina bending and local buckling crushing modes. Fracturing of the laminates is the major contributor for the energy absorption of the crushing process.

Often conducting a full scale experiment is an expensive affair. Hence an alternative cost effective method to assess the energy absorbing capability is very important. The numerical simulation using finite element technique has been adopted in many cases to study the energy absorption. The static and dynamic axial collapse of CFRP tubes were well studied numerically in [10]. The numerical energy assessment of hybrid tubes made of pultruded tube overwrapped by braiding were studied by and Han [8] and his co-workers. The peak load and the corresponding energy absorption characteristics of square sandwich composite vehicle hollow body shells were discussed in [11]. However in all these cases, the modeling of delamination which cause the split of outer and inner petals of the tubes during the crushing are not considered. Hence in this investigation, an attempt was made to study the deformation characteristics of the composite tube using delamination approach.

Many studies [5, 12] demonstrated that fibre orientation along the axis of the tube absorbed more energy than other orientations. In connection with that the pultruded tubes were chosen for this study. Circular and square tubes with glass polyester and vinylester were considered for our investigation. The energy absorption characteristics of these tubes were studied experimentally. For numerical simulation, cohesive elements along with the seam elements were employed to achieve the appropriate deformation pattern of the composite tubes. The energy absorption levels, deformation pattern and the deformation length are discussed.

2. MATERIALS AND EXPERIMENTAL METHODS

2.1. Composite tubes and material data

All the tubes which were used for the tests are manufactured by pultrusion process (M/s EXEL, Belgium). Tube laminates were made with continuous 0° orientation fibres. To get the better surface finish the outer and inner layers were made up of random short glass fibres with approximate thickness of 0.1- 0.2mm to get a uniform surface finish (Figure 1). Different test specimens SP1 and SP2 for square and CP1, CP2, CV1 and CV2 for circular were analyzed experimentally. The nomenclatures of the tubes are as follows. The first letter represents the profile of the tube, "S" represents square and "C" represents circular. The second letter represents the type of matrix used. The letter "P" represents the polyester and "V" represents the vinylester matrix. The third letter indicates the type of triggering, the number 1 represents type 1 and 2 represents the type 2. The type 1 is the 45 deg chamfering around the edges of the tubes and the type 2 is tulip pattern with an included angle between the edges of 60 deg. The two triggering profiles are shown in Figure 2 (a) and (b). The motivation to choose these types was, for type 1 profile the initial contact of the impactor will be uniform along the circumference of the tube at the time of impact, whereas in the case of type 2 the contact will take place at the sharp edges of the specimen. The first mechanism would enhance uniform circumferential interlaminar cracks causing the uniform delamination. In case of the triggering type 2, the initial cracks develop at the sharp edges of the tube which contact the impactor. The tolerances in the tube thickness were checked. The

standard deviation of thickness was found 0.05, 0.09 and 0.04 mm for SP, CP and CV series respectively.

Hamada and Ramakrishna [13] worked on the progressive crushing of circular cross sectional tubes and proved that, tubes having a t/D ratio less than 0.015 will fail catastrophically (t – thickness of the tube; D – diameter of the tube). However the tubes with t/D ratio in the range 0.015 to 0.25 will crush progressively. So the t/D ratio of the circular tube was chosen 0.06 and 0.07 for glass polyester and glass vinylester tubes respectively. For square tubes, a t/W ratio of (W- width of the tube) 0.075 was chosen.

Figure 1: Test specimens

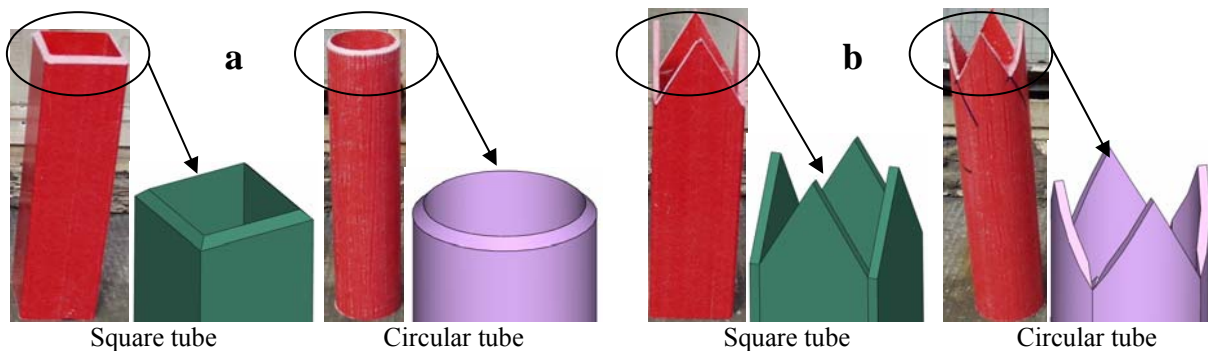| Square tube | Circular tube | Square tube | Circular tube |

Figure 2: (a) Triggering Type 1 (b) Triggering Type 2

To achieve the progressive failure of the composite tubes, the linear density (mass per unit length) of the tube was chosen as recommended in [14]. The details of the tube geometry, fibre, matrix, tube dimensions, linear density and the corresponding volume fraction are mentioned in Table 1.

Table 1: Dimensional and material details of the tube series

S.No	Tube series	Cross section	Fibre	Matrix	Dimension (mm)	ρ_{linear} (g/mm)	Volume fraction
1.	SP	Square	Glass	Polyester	Outer width = 60 Thickness =4.5	1.81	Matrix (V_m) = 49.2 % Fibre (V_f) = 50.8 %
2.	CP	Circular	Glass	Polyester	Outer diameter =50 Thickness =3	0.66	Matrix (V_m) = 51.7 % Fibre (V_f) = 48.3 %
3.	CV	Circular	Glass	Vinylester	Outer diameter =38 Thickness =3	0.60	Matrix (V_m) = 49.7 % Fibre (V_f) = 50.3 %

2.2. Experimental setup

All the tests have been performed with the impact test facility shown in Figure 3 and 4. The main horizontal supporting structure is attached to a vertical wall. The horizontal supporting structure is attached with the vertical guide where the impactor slides. A scale was fixed parallel to the guiding rail to measure the height of the impact. The maximum drop height for

the impactor is 12m. However for this experiment the impact height was limited up to 10m. The bottom of the vertical sliding support is fixed to a 20mm thick steel plate to withstand the total impact force during the impact test. The impact base plate setup was placed over the massive concrete basement.

2.3. Data acquisition system

The system was equipped with a high speed camera (Photron APX RS 250K) with maximum frame rate of 250,000 fps (Figure 5). This was coupled with a computer which records the images at specified instance of time during the impact event. The tracking area by the camera covered the entire impact basement. A special metal – hybrid lamp was used to maintain the light intensity at the area of impact basement.

To capture the deformation event of the composite tubes, a frame rate of 2000 fps with screen resolution of 384 x 400 was chosen. Markers were placed on the impactor as well as on the test specimen for digital image tracking. About a half meter height was covered by the focus lens of the high speed camera, from the basement of the impact system. To calculate every position of the impactor with respect to impact time, this focused vertical distance was adjusted to 300 pixels on the screen vertically. The position of the impactor was recorded at every instance of impact time. From this data the corresponding velocities were calculated. Due to the clearance between the impactor guides and the impactor, a small change in the horizontal velocity was observed. However compared to the magnitude of the vertical velocity it is negligible.

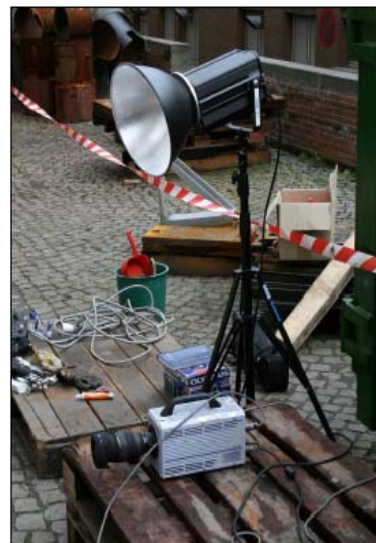Figure 3: Experimental setup   Figure 4: Impactor   Figure 5: High speed camera

3. Experimental results and Discussion

3.1. Failure pattern

The progressive failure study of different types of composite tubes was investigated with different impact velocities. Each set of composite tubes consists of square (SP1 and SP2) and circular tubes (CP1, CP2, CV1 and CV2). They were tested with different drop heights which correspond to 9.3, 12.4 and 14 m/s initial impact velocities. A sample of a square composite tube which has undergone the different phases of deformation is shown in Figure 6.
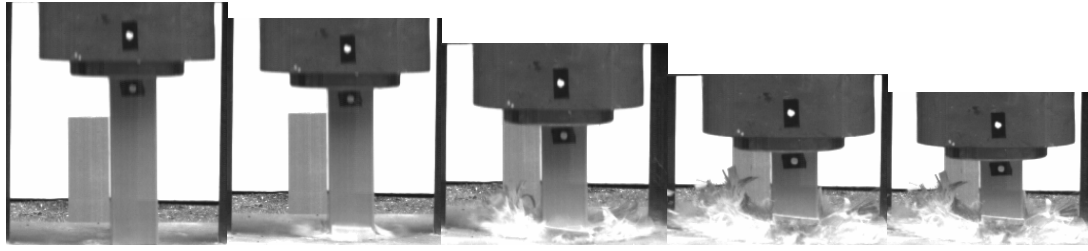
4

Figure 6: Different phases of square tube crushing.

3.1.1 Square tubes

For both types of square tubes (SP1 and SP2) after the circumferential delamination, the primary longitudinal cracks were developed along the corners. The major impact energy of both types of tubes was exhibited by lamina bending followed by the breakage of matrix bonds. The separation of plies from each other was directly proportional to the number of interlaminar cracks which developed during the impact process. The complete surface delamination of inner and outer random fiber mat was observed from the core fibres. The decohesion of outer and inner skin is due to the uneven distribution of the bonding strength along the thickness of the tube. The lamina of each face of the square tube acted as a cantilever beam, which absorbed considerable amount of impact by its bending mode. During the crash event, the bending angle of each side lamina was observed 90° for all square tubes. However due to the higher stiffness of each lamina the angle was gradually reduced when the impact force magnitude reached to zero (Figure. 7 and 8). This mode was observed different from the previous reported modes [10] where all the laminae deformed permanently for 90°. However the inner laminae have undergone permanent bending as well as tearing mode (Figure. 7 (a) and (b)). Unlike triggering type 1, the triggering type 2 exhibited permanent bending of the laminae due to their lesser stiffness. This can be clearly noticed from the Figure- 8(a) and (b).

Figure 7 (a & b): Failure pattern of SP1 series (c) Cut section of the tube

Figure 8 (a & b): Failure pattern of SP2 series (c) Cut section of the tube

3.1.1 Circular tubes

Similar to square tubes, in all the varieties of circular tubes (CP1, CP2, CV1 and CV2) the petals were formed due to the circumferential delamination and consequent by axial cracks parallel to the axis of the tube. The uniform geometry of the circular tube facilitated to form more axial cracks and thus more petals were formed. The major amount of impact energy was absorbed due to the increasing number of longitudinal cracks and subsequent bending of the laminates [15]. This phenomenon was clear in all the cases in which the specific energy absorption of the circular tube was more than the square tube (Figure 12 –a). Unlike the square tubes irrespective of the triggering and fibre fraction volume, the bending angles of the laminates were noticed greater than or equal to 90° (Figure 9 and 10). The cut section of the square and circular tubes proved that, the circumferential delamination took place at the mid of the thickness (Figure 7 (c), 8 (c), 9 (c) and 10 (c)).
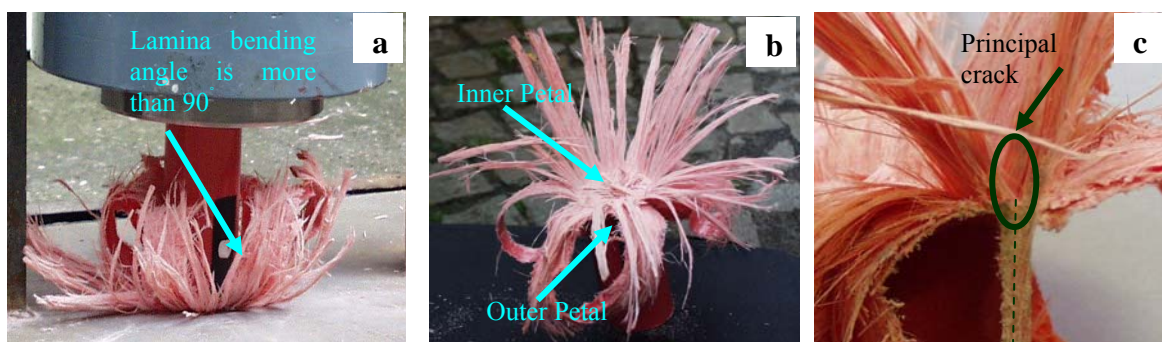

Figure 9 (a & b): Failure pattern of CP1 and CP2 series (c) Cut section of the tube

Figure 10 (a & b): Failure pattern of CP1 and CP2 series (c) Cut section of the tube

3.2. Specific energy absorption

In order to determine the consistent value of deformation length of the tubes, two specimens were tested in each category. The average deformations of the tubes were considered to calculate the specific energy absorption of each case. The average specific energy absorption (SEA) was calculated based on the formula below and the corresponding energy dissipation of all series of tubes for the initial impact velocity 9.3 m/s are shown in Figure 11.

$$\text{Specific Energy absorption (SEA)} = \frac{E_d}{d * \rho} \text{ kJ/kg} \qquad (1)$$

where, E_d is the total dissipated energy by the tube (kJ)
d is the deformation length of the tube (m)
ρ is the linear density of the composite tube (kg/m)

The dissipated amount of energy with respect to the deformed length of the each series of tubes for the initial impact velocity 9.3 m/s is shown in Figure 11. As discussed earlier in section 3.1, due to the uniform geometry the circular tube yielded more axial cracks. This larger number of axial cracks attributed to higher specific energy absorption. Both the varieties of the circular tube with polyester and vinylester exhibited higher value of specific energy absorption than the square tubes. The effect of triggering on SEA is also clearly seen from Figure 12. In case of circular tubes, the triggering type 1 absorbed more energy than the triggering type 2. This is due to the fact that, during the impact event controlled circumferential delamination takes place along the circumference of the tube. In case of square tubes the triggering type 1 exhibited more SEA than triggering type 2, however the difference was less. The matrix effect on SEA for CP and CV series with triggering type 1 was negligible. However in triggering type 2 there was a significant difference. The CV series absorbed approximately 30% more SEA over CP series (Figure 12(a)). The Figure 12(b) shows the effect of strain rate on SEA.
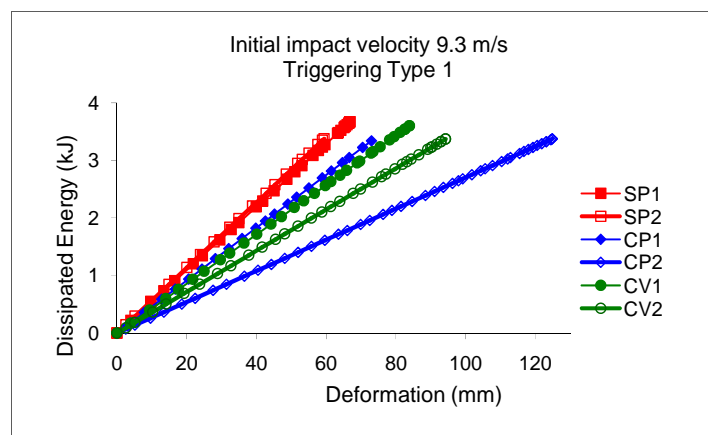

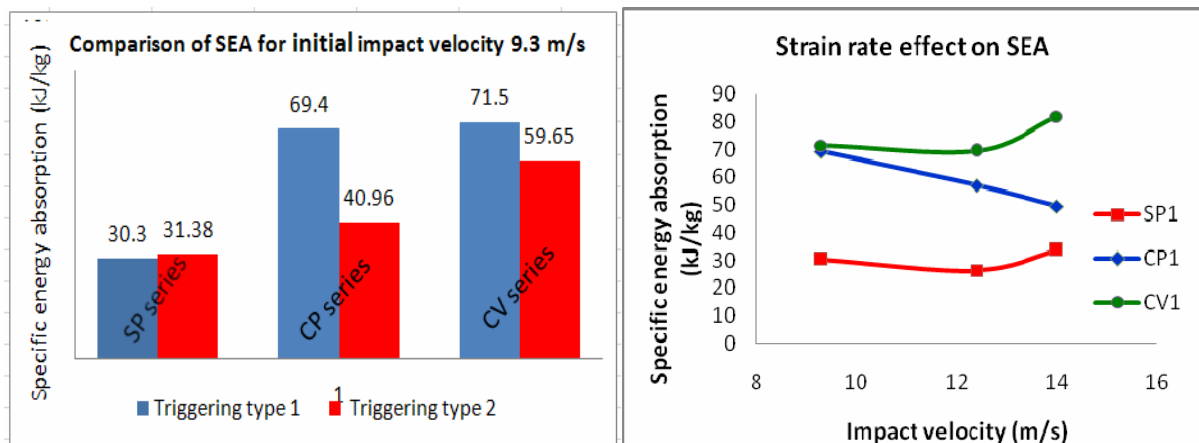
Figure 11: Energy dissipation for each series of tube

Figure 12: (a) Comparison of SEA   (b) Strain rate effect on SEA

4.0. NUMERICAL SIMULATION AND RESULTS

4.1. Numerical modeling

7

The experimental results provided the evidence of delamination taking place at the mid of the tube thickness. Hence the tube was divided into two equal layers of shell elements representing the outer and inner laminae. The meshed shell elements were located at the centre of the thickness of each layer of 0° laminate. The undamaged orthotropic plane stress material response was specified directly by elastic stiffness matrix (E_{11}= 33.5 GPa; E_{22}= E_{33}= 8 GPa; ν_{12}= ν_{13}= 0.29; G_{12}= G_{23}= 5.5 GPa)   In ABAQUS Explicit V6.7 [16, 17], the anisotropic damage model is based on the work of [18]. This damage model considers the following four failure modes, (i) fibre rupture in tension (ii) fibre buckling and kinking in compression (iii) matrix cracking under transverse tension and shearing and (iv) matrix crushing under transverse compression and shearing. The same damage model was used for all the analysis. To model the delamination between the outer and inner lamina of composite tubes, a layer of cohesive elements was added at the mid of the two shell layers. The mechanical properties of the cohesive layer which represents polyester and vinylester were adopted from [19]. The traction separation constitutive response was used which ensures that nominal strains are equal to the relative separation displacement of the cohesive layer. Pure master and slave contact was used between the shell layers and the cohesive elements. To represent the axial crack along the length of the tube, the seam elements were assigned to the predefined location along the axis of the tube. ABAQUS places duplicate nodes along the seam and they are free to move at the time of crack growth.

In the modeling of the axial crushing, the one end of the tube was attached to the rigid plate using "Tie" constraints. The impactor mass of 68.85 kg and the initial impact velocity were assigned to the rigid plate. The impact base plate was also modeled as a rigid plate.

4.2. Comparison of results

All varieties of tubes were analyzed for three different axial crushing velocities 9.3, 12.4 and 14 m/s. The deformation patterns of square composite tubes (SP1 and SP2) and the circular tubes at different times during the impact (CP1 and CP2) are shown in Figure 13 to 15. The sequence of the deformation pattern for all the tubes matched very well with the experimental results. As an example the comparison of deformation lengths with the experimental results for the case SP1 is presented in Figure 16.
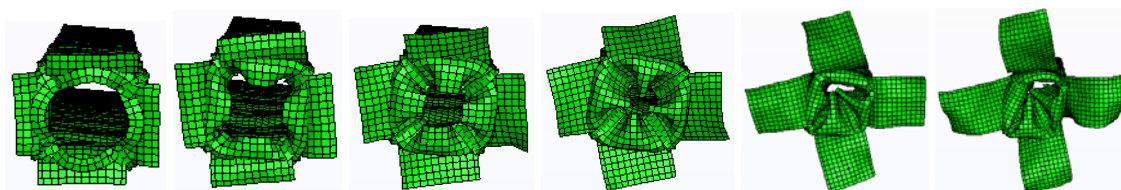

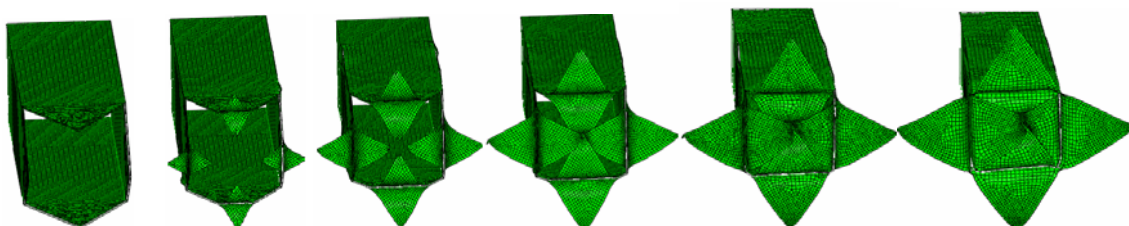
Figure 13: Deformation sequence of SP1 series

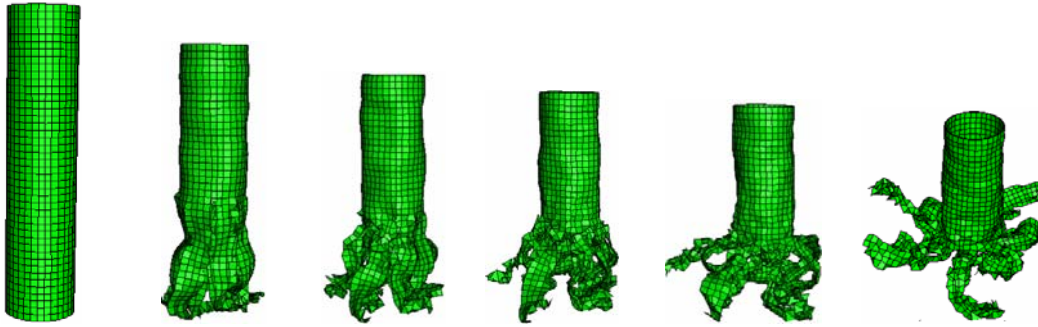Figure 14: Deformation sequence of SP2 series
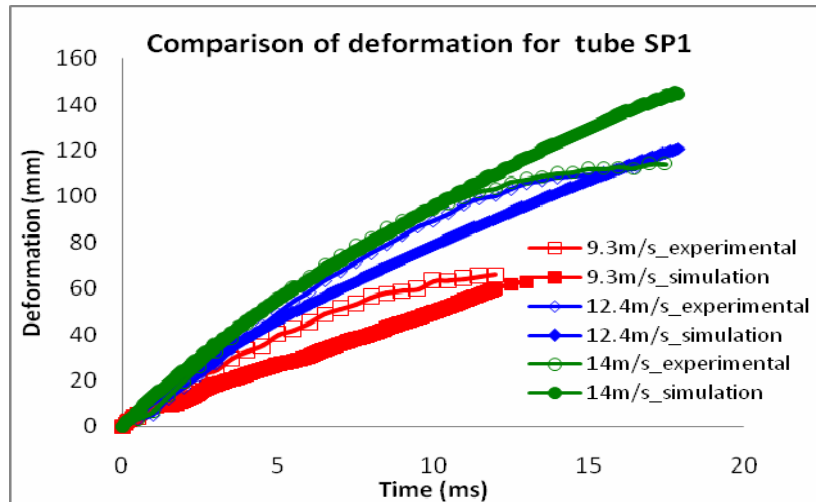
Figure 15: Deformation sequence of CP1 series

Figure 16 : Comparison of deformation for tube SP1

5. CONCLUSION

In this study, the impact energy absorption characteristics and its crushing mechanism using glass fibre - polyester and glass fibre – vinylester square and circular tubes with different thickness were investigated. The different t//D ratio were chosen to achieve the progressive failure of the tubes. Numerical simulation was conducted to study the energy absorption especially the deformation pattern of the tubes. The general conclusions from all tests which were conducted are as follows:

- In all cases, the circular tube was found to absorb more energy than the square tubes.
- Out of the two types of triggering, the triggering type 1 (45° chamfering around the edge of the tube) absorbed more energy than the triggering type 2 (tulip pattern). For circular tubes with t/D ratio of 0.06 and 0.078 yielded 40% and 17% increase in SEA respectively. In case of square tubes there was a negative effect observed due to the triggering type 1, however the difference in SEA was small.
- It was found that the SEA of tubes with glass vinylester was more than the tubes with the glass polyester.
- For tube series SP and CV the increasing trend in SEA was observed with increasing impact velocity. However in CP series the SEA decreased with increasing impact velocity. More tests have to be performed for the consistency of this case.
- Numerical simulation using cohesive and seam elements predicted the correct failure pattern of the composite tubes. The corresponding deformation lengths were comparable with the experimental results.

REFERENCES

1- D.Thambiratnam, G.N., *Energy absorption and performance of a vehicle impact protection system.* Structures under SHOCK AND IMPACT, 2000. **VII**: p. 229-237.

2- Qiao, J.S., J.H. Chen, and H.Y. Che, *Crashworthiness assessment of square aluminum extrusions considering the damage evolution.* Thin-Walled Structures, 2006. **44**(6): p. 692-700.

3- Mamalis, A.G., et al., *Crashworthy capability of composite material structures.* Composite Structures, 1997. **37**(2): p. 109-134.

4- Bolukbasi, A.O. and D.H. Laananen, *Energy absorption in composite stiffeners.* Composites, 1995. **26**(4): p. 291-301.

5- Farely, G.L., *Energy absorption in composite materials* Journal of Composite Materials, 1983. **17**: p. 167.

6- Hamada, H., S. Ramakrishna, and H. Satoh, *Crushing mechanism of carbon fibre/PEEK composite tubes.* Composites, 1995. **26**(11): p. 749-755.

7- Ramakrishna, S. and D. Hull, *Energy absorption capability of epoxy composite tubes with knitted carbon fibre fabric reinforcement.* Composites Science and Technology, 1993. **49**(4): p. 349-356.

8- Han, H., et al., *A numerical study on the axial crushing response of hybrid pultruded and +/-45[degree sign] braided tubes.* Composite Structures, 2007. **80**(2): p. 253-264.

9- Ramakrishna, S., *Microstructural design of composite materials for crashworthy structural applications.* Materials & Design, 1997. **18**(3): p. 167-173.

10- Mamalis, A.G., et al., *The static and dynamic axial collapse of CFRP square tubes: Finite element modelling.* Composite Structures, 2006. **74**(2): p. 213-225.

11- Mamalis, A.G., et al., *Crushing of hybrid square sandwich composite vehicle hollow bodyshells with reinforced core subjected to axial loading: numerical simulation.* Composite Structures, 2003. **61**(3): p. 175-186.

12- Farely, G.L., *Effect of fibre and matrix maximum strain rate on the energy absorption of composite materials.* Journal of Composite Materials, 1986. **20**: p. 322.

13- Hamada, H. and S. Ramakrishna, *Scaling effects in the energy absorption of carbon-fiber/PEEK composite tubes.* Composites Science and Technology, 1995. **55**(3): p. 211-221.

14- Thronton, P.H.E., P.J, *Energy absorption in composite tubes.* Journal of Composite Matter, 1982. **16**: p. 521-545.

15- Solaimurugan, S. and R. Velmurugan, *Progressive crushing of stitched glass/polyester composite cylindrical shells.* Composites Science and Technology, 2007. **67**(3-4): p. 422-437.

16- *ABAQUS User manual.* ABAQUS, Inc. and Dassault Systèmes 2007.

17- *ABAQUS Theory manual.* ABAQUS, Inc. and Dassault Systèmes, 2007.

18- Hashin.Z, R.A.a., *A fatigue failure criterion for fiber reinforced materials.* Journal of Composite Materials, 1973. **7**: p. 448.

19- Warrior, N.A., et al., *Effect of resin properties and processing parameters on crash energy absorbing composite structures made by RTM.* Composites Part A: Applied Science and Manufacturing, 2003. **34**(6): p. 543-550.